

Phonon bound state and critical limit of soliton motion in ferroelectrics

A. BISWAS^a, K. CHOUDHARY^a, A. K. BANDYOPADHYAY^{a,b*}, A. K. BHATTACHARJEE^c, D. MANDAL^c

^aDumkal Institute of Engineering & Technology, W. B. University of Technology, Dumkal, Dist: Murshidabad, India

^bCalcutta Institute of Engg. & Management, W.B. University of Technology, 24/1A C G Road, Kolkata-700040, India

^cDept. of Electronics and Communication Engineering, N. I. T., Durgapur West Bengal-713209, India

In the continuum limit of our discrete Hamiltonian, nonlinear Klein-Gordon equation was derived that gave rise to slower *tanh* and faster *sech* soliton solutions while doing the stability analysis as a function of both spatial (x) and time (t) variables. For these solitons a critical field was worked out at non-zero polarization and field so that the soliton motion can prevail in the ferroelectric devices. This non-dimensional critical field gives rise to the applied field (E_{max}) for a nano device of 100 nm thickness that shows interesting behavior against Landau coefficient, which depends on impurity contents. Again, in the discrete case, discrete breathers have been observed due to nonlinearity. Hence, to investigate the above phenomenon in nano-devices, we take two-phonon bound states, i.e. quantum route and calculate various parameters, which when plotted against Landau coefficient for various E_{max} shows a transition behavior around a particular impurity content indicating easier switching hitherto not done. This new approach reveals an interesting aspect for nanoelectronic device manufacture based on ferroelectrics.

(Received June 5, 2011; accepted September 20, 2012)

Keywords: Phonon Bound State, Critical Soliton Motion, Ferroelectrics

1. Introduction

Below Curie temperature, certain perovskites show important ferroelectric behaviour, which have a wide range of applications, notably in non-linear photonic devices and as non-volatile memory [1-5]. Previously, a Klein-Gordon (KG) equation has been derived based on a discrete Hamiltonian [6], and also on a continuum limit [7] in important photonic materials such as lithium niobate and lithium tantalate. The Landau-Ginzburg free energy functional has been taken as the potential energy in both cases in terms of two-well nonlinear potential formulations. The ‘analytical solution’ of K-G equation gave both low velocity (*tanh*) and high velocity (*sech*) solitons in such photonic materials. An extensive description of the behavior of different solitons has been given by Dauxois and Peyrard [8]. The stability of these solitons, i.e. up to what field such solitons exist, has been worked out in order to find a critical field, which has not been attempted so far in actual photonic crystals with implications for device applications [6].

The ferroelectric behaviour is mostly guided by the formation of domains and domain walls and their rotation with the field. Several impressive studies have been made by Vanderbilt et al [9,10] on the ab initio calculation of domain growth kinetics and domain wall movement, and the apparent domain width was worked out on a time-averaged scale, which are based on rather wide spatial excursions taken by such domain walls. In this paper, although the interplay of domain width and critical field is not explicitly elaborated, it is assumed that impurities create some sort of difficulty in the domain rotation, or

rather with an increase in domain width (i.e. a decrease of domain wall width) there is an increase of the coercive field (E_c) [11-15]. In an important work on simulation of cracks in ferroelectrics, it was found that both the hysteresis and coercive field were greatly affected by the ratio of the characteristic length to domain wall width, and hence exemplifying the greater role of domains and domain walls [16]. The preparation techniques of different ferroelectric materials may also affect the properties in terms of distribution of defects (or impurities) in the domain walls [17] that was also shown to be important by Scott and co-workers [18,19]. In a recent work by Bandyopadhyay and co-workers for the effect of damping on switching behaviour, the importance of domains and domain walls was also shown [20].

A prominent feature of domain wall is explained by a soliton solution, i.e. nonlinear localized traveling waves that are robust and propagate without change in shape, giving the polarization profile and the distribution of the elastic strain across the domain wall. On the other hand, DBs are discrete solutions, periodic in time and localized in space, and whose frequencies extend outside the phonon spectrum. As the existence of DB has already been shown in case of a discrete Hamiltonian [6,11], it was also considered very important to show the physical overview of such classical breathers in 3-dimensions in lithium niobate type of inhomogeneous ferroelectrics [21] as a function of some important controlling parameters, even to the extent of revealing the presence of bi- and tri-breathers that has not been attempted in Ref [11]. An extensive research on dynamics of domain walls in elastic ferromagnets and ferroelectrics was done by Kivshar et al.

[22] by employing sine-Gordon equation coupled to D'Alembert equation for interacting longitudinal and transverse acoustic waves for 'localization' in nonlinear discrete lattice. For dielectrically soft matrix, Bussman-Holder et al. [23] studied Relaxor ferroelectrics with intrinsic inhomogeneity. Here, some points need to be mentioned about localization.

Localization in a system is attributed either to its impurity/disorder or to its nonlinearity [24]. This phenomenon in terms of Anderson localization has been implemented in details in many types of device applications. As the nonlinearity arises in ferroelectrics in terms of P - E hysteresis due to the rotational movement of the discrete domains and domain walls, it also gives rise to the localization. DBs seem to be quite versatile in managing localized energy, i.e. in targeted energy transfer or trigger mechanism [25]. They can transport this energy efficiently by engaging the lattice in their motion after DBs are formed, and moreover, under specific circumstances they can transfer this energy in selected lattices [26,27]. Combining these facts from model as well as some more general studies, it can be written that DBs in ferroelectrics could in principle act as an able energy manager [28]. As we are primarily concerned with the explanation of critical soliton motion through two-phonon bound state, i.e. quantum route, some of the important works about the phonons are listed below in a non-exhaustive literature search.

Corso et al. did an extensive study of density functional perturbation theory for lattice dynamics calculations in a variety of materials including ferroelectrics [29]. They employed a nonlinear approach to mainly evaluate the exchange and correlation energy, which were related to the non-linear optical susceptibility of a material at low frequency [30]. The phonon dispersion relation of ferroelectrics was also studied extensively by Ghosez et al [31,32]; these data were, however, related more with the structure and metal-oxygen bonds rather than domain vibrations or soliton motion. In a very interesting work, a second peak (as previously observed by Krishnan in the Raman Spectra) was interpreted by Cohen and Ruvalds [33] as evidence for the existence of 'bound state' of the two phonon system and the repulsive anharmonic phonon-phonon interaction which splits the bound state off the phonon continuum was estimated for diamond.

A femtosecond time-domain analog of light-scattering spectroscopy called impulsive stimulated Raman scattering (ISRS) is a very useful technique that has been used by Nelson and co-workers [34] in dealing with the anharmonic vibrations in both lithium niobate and lithium tantalate crystals (see the references therein). A powerful technique, such as molecular-dynamics simulations of vibrational wave packets, was used by Phillpot and co-workers [35] to study the scattering of longitudinal-acoustic modes and predicted that the presence of gaps in the phonon spectrum of thin high-symmetry nanowires will result in a complete reflection of phonons at the interfaces.

A brief account is given here on phonon bound state or breather state. Despite our work on discrete breathers [11], so far the soliton motion in ferroelectrics has been explained classically, thereby making us think about quantum route, which has been attempted in the present work. Hence, to explain the dependence of criticality of soliton motion on nonlinearity, it is relevant to consider detailed information on phonons [36] and their bound state concept, which is sensitive to impurity content in the lattice. Let us consider that the phonons in one sublattice may hop from one domain to another adjacent domain. This hopping might have some consequences with the change of impurity content in the entire crystal that has a relation with the nonlinearity parameter, thereby the 'hopping strength' can be directly related to the Landau coefficient [27]. It is determined by finding the phonon energy gap in the energy-spectrum by analyzing the quantum-breather state [37,38] (see references therein) or phonon bound state. Thus, the objective of this paper is to explore how nonlinearity parameter influences the soliton motion or its criticality by quantum calculations hitherto not done. Therefore, the hopping strength of phonon and thus the phonon energy gap are derived from the quantized model of the ferroelectrics. In this new approach, the calculations of various parameters related to phonon bound states, or breather states, have been made against Landau coefficients i.e. at different impurity contents, to highlight the quantum origin of this phenomenon in ferroelectrics, which have implications in various ferroelectric devices including many nano devices.

The paper is organized as follows: in Section 2, brief theoretical background is given for both the continuum limit for critical soliton motion and phonon bound state for relevant parameters, and in Section 3 important results are shown whereby the dependence of this critical field on nonlinearity parameter for the continuum case (Section 3.1) as well as the relation of different parameters concerning phonon bound state on nonlinearity (Section 3.2). Here the results are shown for lithium niobate ferroelectrics against nonlinearity, i.e. with wide range of impurity contents, and also for some other ferroelectrics where the nonlinearity parameters are known. In Section 4, the conclusions are given.

2. Theoretical aspect

Here, first of all, we discuss the theoretical aspect of our discrete Hamiltonian in the continuum limit to find out the critical value for soliton motion and then deal with phonon bound state or discrete breather state to explain the possible dependence of criticality on the Landau coefficient through quantum route.

2.1. Continuum Limit:

The nearest neighbor domains [i.e. the polarization in the i -th domain (P_i) with that in the $(i-1)$ th domain (P_{i-1})] were taken to interact by a harmonic potential with a phenomenological spring constant k so that the resulting

discrete Hamiltonian for the polarization is given by [6]:

$$H = \sum_{i=1}^N \left(\frac{1}{2m_d} \right) p_i^2 + \sum_{i=1}^N \frac{k}{4} (P_i - P_{i-1})^2 + \sum_{i=1}^N \left(\left(-\frac{\alpha_1}{2} P_i^2 + \frac{\alpha_2}{4} P_i^4 \right) - EP_i \right) \quad (1)$$

Here, α_1 and α_2 are Landau coefficients that have important implications in the formation of discrete breathers (see later) and E is the applied field. The momentum (p_i) can be defined in terms of order parameter (P_i) as:

$$p_i = \frac{\partial}{\partial t} \left(\frac{m_d}{Q_d} P_i \right) = \left(\frac{m_d}{Q_d} \right) \dot{P}_i \quad (2)$$

where m_d and Q_d are two inertial constants. Eq. (1) can be approximated by a continuum treatment through Taylor expansion. In this limit, expressed in dimensionless units, for the evolution of polarization (P) with both space (x) and time (t), Eq. (1) yields a nonlinear Klein-Gordon equation with a non-dimensional damping term as [6]:

$$\frac{\partial^2 P}{\partial t^2} + \bar{\gamma} \frac{\partial P}{\partial t} - \bar{k} \left(\frac{\partial^2 P}{\partial x^2} \right) - (\bar{\alpha}_1 P - \bar{\alpha}_2 P^3) - E = 0 \quad (3)$$

for the dynamics of polarization $P(x,t)$. All the terms in Eq. (3) with their possible range of values are given in Ref. [21]. Eq. (3) is obtained by taking $\alpha_1 = \alpha_2/P_s^2$ and $\bar{\alpha}_1 = \bar{\alpha}_2 = \bar{\alpha} = (\alpha_1 P_s)/E_c$ [6,11]. Here, the interaction and damping terms are defined as:

$$\bar{k} = \frac{kP_s}{2E_c} \quad (4)$$

$$\bar{\gamma} = \frac{\gamma P_s}{t_c E_c} \quad (5)$$

where γ is a decay constant relating the loss of polarization due to internal friction during its motion in the system of domains.

It should be noted that in Eq. (3), since the non-dimensional E contains the switching field E_c that is again dependent on the impurity contents in an inhomogeneous ferroelectric material [11,14], our above treatment thus embodies the impurities. Therefore, the study of the critical field for the stability of the solitons as a function of the impurity content is relevant in a real inhomogeneous system. Equivalently, as E_c directly varies with impurity [14] and it is inversely proportional to the Landau coefficient as mentioned above, we will operate through the latter to give a better description of phonon bound state (see later), as it is dependent on nonlinearity. Based on the above K-G equation, a stability analysis for the existence of the solitons was done in an actual situation for photonic

device applications where $E \neq 0$ and $\bar{\gamma} \neq 0$. In this case, a situation is described in order to see under what condition the soliton exists in our ferroelectric system, such as lithium niobate:

Let us do a transformation of variables with θ_1 as:

$$\theta_1 = \frac{x - \sqrt{\bar{k}} V t}{\sqrt{\frac{2\bar{k}}{\bar{\alpha}} \sqrt{1-V^2}}} \quad (6)$$

where V is a component of the soliton velocity. Let us also put

$$\frac{dP}{d\theta_1} = \phi \quad (7a)$$

$$\frac{d^2 P}{d\theta_1^2} = \frac{d\phi}{d\theta_1} = -2(P - P^3) - V_1 \phi - E_2 \quad (7b)$$

where,

$$V_1 = \left(\frac{\sqrt{2}}{\sqrt{\bar{\alpha}}} \right) \frac{\bar{\gamma} V}{\sqrt{1-V^2}} \quad (8)$$

$$E_2 = \frac{2E}{\bar{\alpha}} \quad (9)$$

The stationary points of a system of equations (7) are given by:

$$\phi = 0 \quad (10a)$$

and,

$$\bar{\alpha}(P^3 - P) - E = 0 \quad (10b)$$

For the three real and distinct roots of equation (10b), the following condition has to be satisfied:

$$E^2 < \frac{4(\bar{\alpha})^2}{27} = E_{crit}^2 \text{ (say)} \quad (11)$$

The equation (11) gives rise to:

$$E_{crit} = \frac{2\bar{\alpha}}{3\sqrt{3}} = 135.85 \quad (12)$$

This is the required condition for the existence of the solitons with stationary velocity for our ferroelectric system. At this condition, two of the stationary points of the system of equations (7) disappear, and no soliton exists

for $\left| \sqrt{k} \cdot V \right| < \sqrt{k}$. This could mean that it is related with

a break-up of the double-well potential to a single-well at high electric fields. Here, we also note that how the nonlinearity or, Landau coefficients are important in deciding the critical value of electric field for the existence of solitons in our ferroelectric system. Although not shown here, for the existence of the solitons, the condition (11)

still holds for $\left| \sqrt{k} \cdot V \right| > \sqrt{k}$, i. e. the solitons with higher

velocity also do not exist after this critical electric field. Therefore, from the above description it is clear that the solitons with stationary velocity exist when the magnitude of the field (E) is less than a critical value in ferroelectric materials, such as lithium niobate. Similar condition will also enable us to establish the existence of solitons with stationary velocity for lithium tantalate that is also very important material in opto-electronic devices. This is not derived here to avoid repetition.

The above non-dimensional critical field is calculated for a particular sample by taking $E_c = 40$ kV/cm and $P_s = 0.75$ C/m² [12]. Therefore, from the so-called ‘material parameters, such as E_c and P_s , it is possible to calculate the critical field for our type of photonic crystals with a wide variety of impurity contents (read, E_c). It is also possible to do the same calculation for other ferroelectrics in order to see the effect of impurities/nonlinearity induced modes on the soliton motion in such photonic materials, which are in most cases non-stoichiometric. It may be mentioned that the soliton motion is generally considered at room temperature for device applications. So, we take the room temperature value of P_s as 0.75 C/m² throughout our calculations at different E_c values.

This critical value could be considered as the limit of thermodynamic coercive field that is calculated from the Landau-Ginzburg (L-G) theory for the second order phase transition, which is known to be much larger than the experimentally observed value [6,7]. An attempt to explain this behaviour was made by Kim et al. [12] and Yan et al. [14]. Many authors feel that it could be due to pinning effect of impurities that are present in the near-stoichiometric to congruent crystals that are studied by us, since the thermodynamic coercive field is usually referred to the ‘homogeneous switching’ of the ferroelectrics sample as a whole. Next, to be able to relate the dependence of this critical behavior of soliton motion on nonlinearity, we discuss the application of phonon bound states or discrete breathers state through quantum route with the help of our discrete Hamiltonian.

2.2. Phonon bound state

Eq. (1) gives a general treatment of the mode dynamics in the array, particularly for modes, which are strongly localized over a small number of the domains in the array. For extended modes and modes which are

localized, and slowly range over a large number of consecutive domains. The discrete Hamiltonian (Eq. (1)) can be split as: $\tilde{H} = H_0 + H_1$.

where,

$$H_0 = \sum_i \frac{P_i^2}{2} - \frac{(\alpha_1 + \lambda)P_i^2}{2} + \frac{\alpha_2 P_i^4}{4} - EP_i \quad (13)$$

$$H_1 = -\frac{\lambda}{2} \sum_i P_i P_{i-1} \quad (14)$$

Here, λ is used as an interaction term instead of k as in Eq. (1). Hence, for n -particles or n -levels in the anharmonic potential well, a general basis may be written as:

$$|\bar{n}\rangle = \psi_{n_1}(x_1)\psi_{n_2}(x_2)\dots\psi_{n_f}(x_f) \quad (15a)$$

and

$$\langle \bar{m} | H | \bar{n} \rangle = \langle \bar{m} | H_0 | \bar{n} \rangle + \langle \bar{m} | H_1 | \bar{n} \rangle \quad (15b)$$

The numerical analysis was carried out with Fourier grid Hamiltonian method [39] (1000 grids, 0.006 spacing) to calculate various eigenvalues and eigenvectors. We restrict ourselves to two phonon states, since at the working temperature the number of phonon is less. In order to reduce the computer memory requirement, we take the advantage of translational invariance by Bloch wave

formulation: $|\psi\rangle = \sum_j v_j |\phi_2^j\rangle$. Due to translational

invariance, the eigenstates of H are also eigenstates of the translation operator T , where: $\tau = \exp(iq)$ is its eigenvalue with $q = \frac{2\pi\nu}{f}$ being allowed Bloch wave

number and $\nu \in \left[-\left(\frac{f-1}{2}\right), \left(\frac{f-1}{2}\right) \right]$. Here, τ is the

eigenvalue of T , and f is taken as a renormalizing constant. Thus, we can construct the Bloch states:

$$|\phi_2^j\rangle = \frac{1}{\sqrt{f}} \sum_{s=1}^f \left(\frac{T}{\tau}\right) |10\dots01\dots\rangle \quad (16)$$

With this basis, we can derive the eigenenergies for each given Bloch wave number q from: $H_q |\psi_n\rangle = E |\psi_n\rangle$. Hence, Eq. (15) reduces to:

$$\langle \bar{m} | H | \bar{n} \rangle = \sum_i \delta_{i,i} E_i - C \sum_i [\exp(-ijq) \left(\prod_i \delta_{m_i, n_i} \right) D_{m_i-1, n_i-1} D_{m_i, n_i}] \quad (17)$$

where q is the Bloch-wave number and

$$D_{m_i, n_i} = \sum_i x_i \psi_{m_i}(x_i) \psi_{n_i}(x_i) \quad (18)$$

ψ_{m_i} 's and E_i 's are eigenvectors and eigenvalues obtained from Fourier grid Hamiltonian method. Here, due to symmetric and asymmetric nature of the eigenfunctions $D_{mn} = 0$, if $(m-n) \neq 0$. Hence, for a two-phonons case, the non-zero hopping coefficients are: $D_{01} = D_{10}$, $D_{12} = D_{21}$. The energy gap between the single phonon continuum and a bound state is given by:

$$E_g = E_2 - E_0 - 2(E_1 - E_0) \quad (19)$$

Typical eigenspectra are shown in Fig. 2 and 3. The width of the single-phonon in the eigenspectrum is given by the magnitude of 4σ , where σ is expressed as:

$$\sigma = -\frac{\lambda}{2} D_{01}^2 \quad (20)$$

D_{01} represents the coefficient for zero to single phonon generation. The variation of the single phonon spectrum width (W_{ph}) represents (through $D_{01} = D_{10}$) the creation of a new phonon or annihilation of an existing phonon. Again, the hopping coefficient for a single phonon to become a two-phonon single state or bound state and vice-versa is given by:

$$\mu = -\frac{\lambda}{2} D_{01} D_{12} = -\frac{\lambda}{2} D_{10} D_{21} \quad (21)$$

All the above calculations were done for 51 sites or domains and $\lambda = 12$. More data points could be used in our present simulation, but here we are primarily focused to study nonlinearity/impurity induced critical behavior of soliton motion and its quantum origin. To treat the problem analytically we take the help of second-quantization method as follows:

The basis for just two phonons can be written as:

$$|\Psi_{m,n}\rangle = \sum_{m,n} \Psi_{m,n} a_m^+ a_n^+ |0\rangle, \langle \Psi | \Psi \rangle = 1 \quad (22)$$

where $\Psi_{m,n}$ are the occupation probability amplitudes of the sites m and n respectively and the boson nature of phonons and normalization conditions yield

$$\Psi_{m,n} = \Psi_{n,m} \text{ and } \sum_{m,n} |\Psi_{m,n}|^2 = 1 \text{ respectively. Using}$$

the basis into the Schrodinger equation $\hat{H} |\Psi\rangle = E_V |\Psi\rangle$, where \hat{H} is obtained by quantizing the Hamiltonian in Eq. 1 in a number conserving quantized form with $N \rightarrow \infty$ [40] with

$$\lambda_1 = \frac{\lambda}{(\lambda - \alpha)}, \eta = \frac{2\alpha}{(\lambda - \alpha)} \text{ and } E = 0 \text{ in Eq. 1 leads}$$

to the equation for bi-phonon amplitudes as shown in Eq. 23:

$$\hat{H} = \sum_n a_n^+ a_n + \frac{3}{8} \eta a_n^{+2} a_n^2 + \frac{\lambda_1}{2} \{a_n^+ (a_{n+1} + a_{n-1}) + h.c.\} \quad (23)$$

$$(E_V - 1)\Psi_{m,n} = \frac{3}{8} \eta \Psi_{m,n} \delta_{m,n} - \lambda_1 \left[\sum_{s=\pm 1} \Psi_{m,n+s} + \Psi_{m+s,n} \right] \quad (24)$$

Using lattice periodicity, we may express the amplitudes

$$\Psi_{m,n} \text{ with } l = m - n \text{ as: } \Psi_{m,n} = \frac{1}{\sqrt{N}} \varphi_l e^{iK(m+n)\frac{R_0}{2}},$$

where $K = k_1 + k_2$ represents the total quasi-momentum associated with the motion of the two-phonon center of mass and belonging to the first Brillouin zone. Here, φ is the function of distance between two phonons. As a result of lattice periodicity Eq. 24 may be written as:

$$(E_V - 1)\varphi_l + \frac{3}{8} \eta \varphi_l \delta_{l,0} - 2\lambda_1 \text{Cos} \frac{KR_0}{2} \sum_{s=\pm 1} \varphi_{l+s} = 0 \quad (25)$$

Here, Eq. 25 represents a system of linear algebraic equations for amplitudes φ_l for each l . Expanding φ_l in complex Fourier series:

$$\varphi_l = \frac{1}{\sqrt{N}} \sum_q f_q e^{iqR_0} \quad (26)$$

where f_q 's are Fourier coefficients needed to get the complete series for φ_l and substituting in Eq. 25 yields:

$$[E_V - \xi(K, q)] f_q + \frac{3}{8} \frac{\eta}{N} \sum_{q'} f_{q'} = 0 \quad (27)$$

where,

$$\xi(K, q) = 1 - 2\lambda_1 \text{Cos} \frac{KR_0}{2} \text{Cos} qR_0 \quad (28)$$

Dividing Eq. (25) by $\lambda_1 \text{Cos} \frac{KR_0}{2}$ yields:

$$(\Lambda_K + 2\text{Cos} qR_0) f_q + \Gamma_K X = 0 \quad (29)$$

where, $\Lambda_K = \frac{E_V - 1}{\lambda_1 \cos \frac{KR_0}{2}}$, $\Gamma_K = \frac{3\eta}{8\lambda_1 \cos \frac{KR_0}{2}}$ and

$$X = \frac{1}{N} \sum_{q'} f_{q'}$$

Here, $\xi(K, q)$ represents the energy of two free phonons. The final Eq. 27 is an eigenvalue problem for the two-phonon and is an integral equation for the function of f_q and may be solved using standard numerical techniques. Now, for a two-phonon bound state (TBPS), $\Lambda_K > 1$. Hence, for affixed total quasi-momentum K , the critical α -value or Landau parameter may be calculated as:

$$\alpha_{TBPS} = \lambda \left[\frac{\cos \frac{KR_0}{2}}{E_V - 1} - 1 \right] \quad (30)$$

Hence, for a LiNbO₃ type ferroelectrics, after α_{TBPS} , a branch is separated from the continuum due to corresponding impurity content and has got a critical point for pinning transition. Now, for bound state $m = n$ and the bound state energy (E_{BS}) can be derived as:

$$E_{BS} = 1 + \frac{3\eta}{8} - 4\lambda_1 \cos \frac{KR_0}{2} \quad (31)$$

Taking cosine term as unity and substituting the values of η , λ_1 gives

$$E_{BS} = \frac{\alpha}{\alpha - \lambda} \quad (32)$$

3. Results and discussion

First of all, let us discuss about the results of maximum field to be applied in a device against nonlinearity parameter and then we deal with different parameters related to two-phonon bound state (TPBS) to find out why at a certain value of the nonlinearity parameter, the behavior of phonon energy gap is different.

3.1. Continuum case

The values of E_c and P_s for lithium niobate with a wide variety of impurity contents are taken from Ref. [14], wherein some data of Gopalan et al are also included. The data for lithium tantalate are taken from Tian et al [13]. For photonic device applications, it is important to know the value of the applied electric field so that the soliton motion prevails in the system. If we multiply the non-

dimensional critical field by E_c , we get the maximum value of the applied field (E_{max}) in V/nm to be used in the device. The values of E_{max} in Volts (say, for a 100 nm thin device) are plotted against the Landau coefficient for lithium niobate in Fig. 1. It is seen that after somewhat steeper decrease, it almost saturates towards the congruent side. It is interesting to note that at the α value at around 350-400 corresponding to a value of $E_c = 40 - 44$ kV/cm, the pinning of the domains might start and then becomes stronger making the domain rotation difficult, i.e. quite stiffer, which is accompanied by an increase of E_c values, i.e. increasing impurity content.

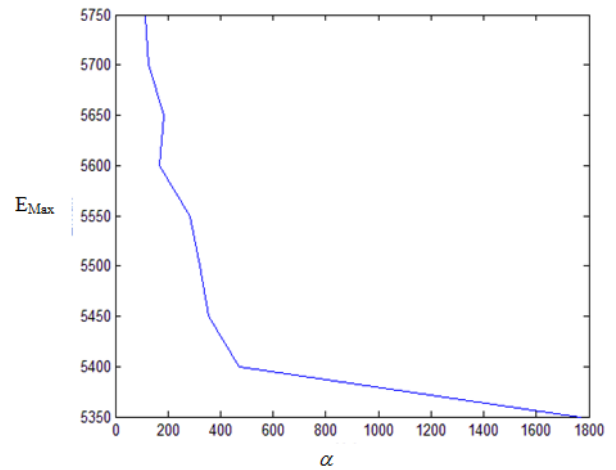


Fig. 1. Maximum applied field value against α showing asymptotic behavior after a particular point corresponding to a value of $E_c = 40-44$ kV/cm

Regarding the change of slope and this optimum point of this curves around 40-44 kV/cm (i.e. impurity content of 0.133 to 0.265 mole %), an explanation can be given as follows:

Domain dynamics [12,13,17] is interpreted by domain reversal phenomenon. Domain reversal takes place in two steps: nucleation and sideways growth. According to Gopalan et al [41] the nucleation rate is almost equal to zero in the low field regime, so the reversal of domain is only initiated in terms of growth of some pre-existing nucleus as evident from many experiments [42,43]. These micro-domains may play the role of nucleus. According to some other works, the motion of the domain wall in near-stoichiometric lithium niobate shows jerky behavior during sideways-growth in the low field regime that was attributed to the pinning role of intrinsic defects [44-46]. Hence, the growth is baffled by the intrinsic defects and can be completed only when the poling field applied on the crystal is large enough for the domain to overcome this difficulty by intrinsic defects. As explained above, the defect structure [11,12] assumes a more important role in the manifestation of different values of E_{max} for different ferroelectrics as a function of impurity. This has been explained in details in Ref. [11, 20].

For lithium tantalate, the values of E_{max} are found to be 27.43-29.98 V/100nm between E_c values: 1.61 kV/cm

(near-stoichiometric) to 210 kV/cm (congruent). Since the impurity contents are not known with precision and moreover due to the paucity of data in the intermediate range, the values are not plotted here. However, for this photonic crystal that is more popular in the device applications due to lower E_c values, the effect of impurity on E_{max} does not seem to be as pronounced between the two extreme values of E_c (i.e. from near-stoichiometric to congruent) as in the lithium niobate. It is assumed that the K-G equation with Landau potential is applicable in such photonic materials. Moreover, there is no significant dependence of P_s on the impurity.

It is pertinent to mention that no strain effect has been included in our analysis, which has been considered by many authors. In our case, it is normalized into the relevant coefficients of the Landau potential, as also done in a previous dynamic analysis of both dark and white solitons [7]. This is also valid in our multiple time scale analysis for different linear and non-linear plane wave excitations and intrinsic localized modes in lithium niobate ferroelectrics, where the impurity dependence of the former is also quite pronounced [11]. This critical field may be explained in terms of symmetry breaking in the Landau potential, whereby it has been observed that at a non-dimensional field value of around 135, the two-well Landau potential gives rise to a single well. At a value of 100, the left hand side well is barely discernible leading to a break-up of the potential, as shown in Fig. 1 of Ref. [47]. It has also been emphasized in the Ref. [47] that as the field is increased, the ferroelectric system tends to go towards a chaotic situation. For the analysis of chaos by K-G equation with an ac driver, a direct proof can be given by the Lyapunov exponent spectrum, if we assume that when $\bar{k} \Rightarrow 0$, i.e. x is very small indicating nano-domains, the K-G equation (Eq. 3) tends to become a heavily damped Duffing oscillator equation [20]. In such a situation, one of the exponents tends to go to the positive domain indicating instability in the soliton motion, i.e. at a critical value of 135.85 (Eq. 12), there is no existence of solitons in our system of ferroelectrics [47]. However, by using the K-G equation based on the Landau potential and the soliton stability, the dependence of the critical field on nonlinearity (read, impurity) is definitely shown in this work with important consequences in the applications of nanoelectronic device manufacture of these ferroelectric materials as photonic devices.

3.2 Different Parameters of TPBS:

For our simulation work, we take just two phonons because at working temperatures the number of phonons are very less. Now, due to nonlinearity in the system, some single phonons form a bound state of phonons, which is a characteristic property of particular ferroelectric material with a specific impurity content. After estimating the E_{max} value, we put these values in the Hamiltonian (Eq. 1) along with corresponding Landau coefficient values, i.e. nonlinearity.

Hence, the eigenspectrum is a signature of the material response. Moreover, we basically observe two important aspects of such plots, namely phonon band gap and delocalized phonon width, which are again characteristic features with a ferroelectric with particular impurity content. Typical eigenspectra with $\alpha = 1767.09$ and $\alpha = 353.42$ are shown in Fig. 2 and Fig. 3 respectively. The transition point with respect to phonon band gap (E_g), i.e. the gap between localized and delocalized phonons, width of delocalized phonon (W_{ph}), i.e. the range of eigenenergy in which the single phonons have been confined and the single to bi-phonon hopping coefficient (μ) are observed in Figs. 4, 5 and 6 respectively.

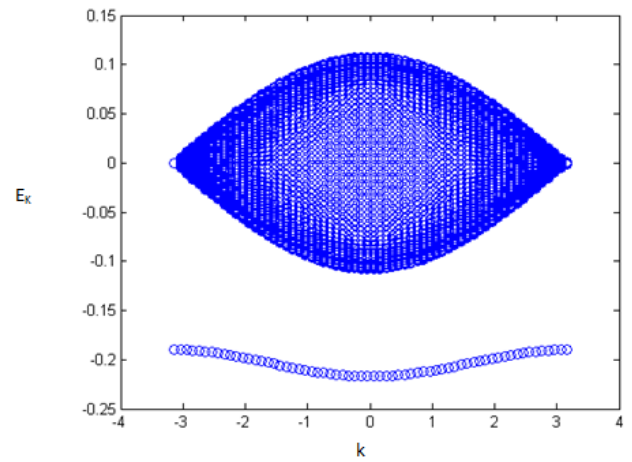


Fig. 2. Typical energy spectrum for $\alpha = 1767.09$ showing localized phonon energy band with a band gap $|E_g| = 0.190$.

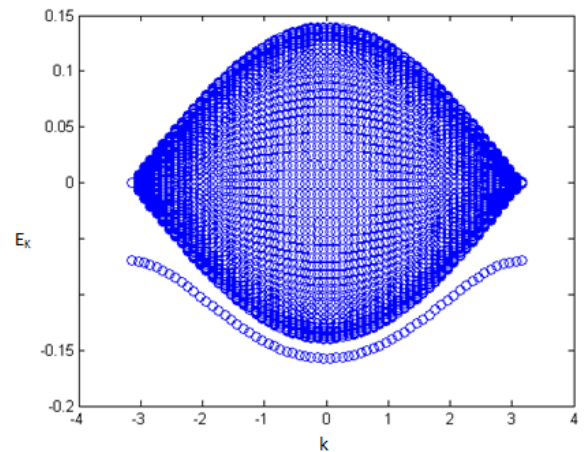


Fig. 3. Typical energy spectrum for $\alpha = 353.42$ showing localized phonon energy band with a band gap $|E_g| = 0.070$.

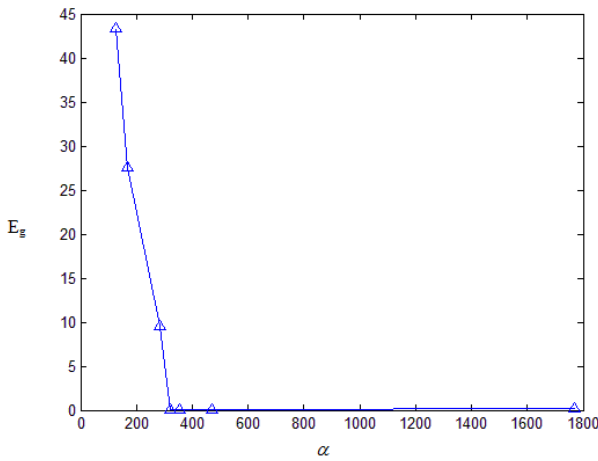


Fig. 4. Energy gap (E_g) vs α showing a critical point around $\alpha = 350$ after which the energy gap becomes almost constant with respect to α .

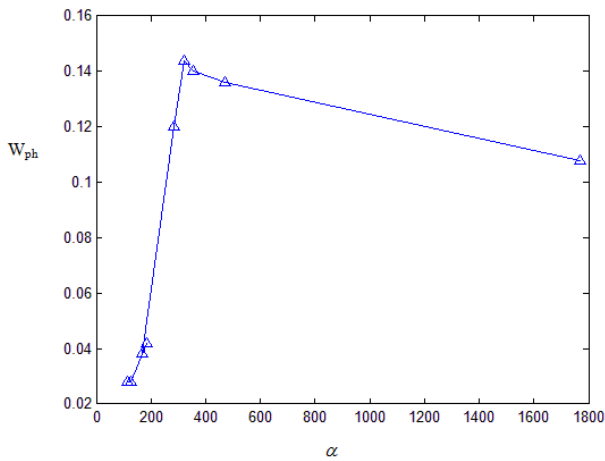


Fig. 5. Width of single phonon (W_{ph}) vs Landau coefficient (α) showing a critical point.

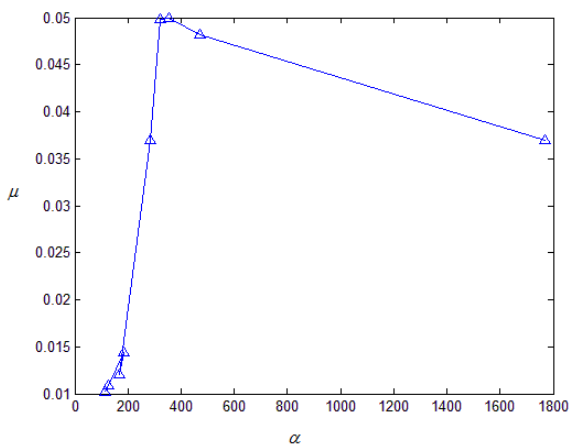


Fig. 6. The hopping coefficient (μ) against the Landau coefficient (α).

In Fig. 4, it is seen that the phonon band gap remain almost constant up to a value of Landau coefficient of about 350 (corresponding to a value of $E_c = 40-44$ kV/cm), and then it increases very sharply towards lower values of α (read, nonlinearity). Due to this sharp increase at this point, the domain rotation could be difficult and a pinning mechanism might start after $E_c = 40-44$ kV/cm. All these acid tests are necessary and almost sufficient tests for this point where phonons can very easily form TBPS after which it becomes increasingly difficult for forming the TBPS due to pinning effect of impurity. In Fig. 5, the width of the single phonon continuum shows a little increase towards lower α value of about 350 and then it decreases steeply towards further lower values. Fig. 6 shows the same general trend for the hopping coefficient (μ) of phonons. Both Fig. 5 and Fig. 6 confirm the behaviour, as manifested in Fig. 4. So, in a practical case of maximum applied field, i.e. when soliton motion will prevail in the system, we confirm a point of nonlinearity, i.e. a particular impurity content or E_c value, where it is easiest to switch with respect to other higher points that should be of great importance for device manufacturers. Although the quantum calculations have been done for LiNbO_3 , it could be claimed that such behavior should also be observed for other ferroelectrics because they more or less follow our generalized discrete Hamiltonian.

4. Conclusions

The stability of the solitons in photonic crystals, i. e. up to what field the solitons exist in such systems, is very important for device applications in terms of estimating the maximum voltage to be applied in a given non-linear photonic device of, say, 100 nm thickness. For a given crystal such as lithium niobate with varying impurity contents, there is a beginning of pinning effect in the initial range of stoichiometry, i.e. higher side of nonlinearity and then there is a sort of difficulty for domain rotations towards the congruent side, when the maximum required voltage keeps on increasing to sustain soliton motion. This point of pinning seems to arise from the two-phonon bound states (TPBS) in lithium niobate ferroelectrics, indicating the origin of this process in terms of quantum discrete breathers that will have an implication on devices. since easier is the formation of TPBS, the easier is switching, as observed with the experimental data [11]. Various parameters related to TPBS have been calculated and then plotted against the Landau coefficient hitherto not done. This approach might be useful to explain some other physical behaviour of ferroelectric materials in terms of TBPS.

References

- [1] H. Fu, R. E. Cohen *Nature* **403** 281 (2000).
- [2] G. I. Stegeman et al *Optics Letters* **29**, 596 (2004)
- [3] A. K. Bandyopadhyay, P. C. Ray *J. Appl. Phys.* **95**, 226 (2004).
- [4] J. F. Scott, *Ferroelectric Memories* (Verlag, Springer). 2000.
- [5] G. Catalan, A. Schilling, J. F. Scott, J. M. Greg *J. Phys: Cond. Matter* **19**, 132201 (2007).
- [6] A. K. Bandyopadhyay, P. C. Ray, V. Gopalan *J. Phys.-Cond. Matter* **18** 4093 (2006).
- [7] A. K. Bandyopadhyay, P. C. Ray, V. Gopalan *Euro Phys. J.-B* **65**, 525 (2008)
- [8] T. Dauxois, M. Peyrard, *Physics of Solitons* (Cambridge University Press, Cambridge). 2006
- [9] B. Meyer, D. Vanderbilt *Phys. Rev. B* **65**, 104111 (2002).
- [10] X. Zhao, D. Ceresoli, D. Vanderbilt, *Phys. Rev. B* **71**, 085107 (2005).
- [11] A. K. Bandyopadhyay, P. C. Ray, L. Vu-Quoc, A. R. McGurn *Phys. Rev. B* **81** 064104 (2010).
- [12] S. Kim, V. Gopalan A. Gruverman, *Appl. Phys. Lett.* **80**, 2740 (2002)
- [13] L. Tian, V. Gopalan, L. Galambos *Appl. Phys. Lett.* **85**, 4445 (2004).
- [14] W. Yan et al *J. Phys. D: Appl. Phys.* **39**, 21 (2006).
- [15] S. Kim, V. Gopalan, K. Kitamura, Y. J. Furukawa *J. Appl. Phys.* **90** 2949 (2001)
- [16] Y. C. Song, R. L. Hu, A. K. Soh *Phys. Scr.* **T129**, 136 (2007).
- [17] S. D. Tsai, M. B. Suresh, C. C. Chou *Phys. Scr.* **T129** 175 (2007)
- [18] J. F. Scott *J. Phys.: Cond. Matter* **18**, R361 (2006).
- [19] M. Dawber, A. Gruverman, J. F. Scott, *J. Phys: Cond. Matter* **18**, L71 (2006).
- [20] P. Giri, S. Ghosh, K. Choudhary, Md Alam, A. K. Bandyopadhyay, P. C. Ray *Phys. Scr.* **83**, 015702 (2011).
- [21] P. Giri, K. Choudhary, A, Sengupta, A. K. Bandyopadhyay and P C Ray *J. Appl. Phys.* **109**, 054105 (2011)
- [22] Y. S. Kivshar, B A Malomed *Phys. Rev. B* **42**, 8561 (1990).
- [23] A. Bussmann-Holder, A. R. Bishop, T. Egami *Europhys. Lett.* **71**, 249 (2000).
- [24] J. W. Fleischer, M. Segev, N. K. Elfremedi, D. N. Christodoulides *Nature* **422**, 147 (2003).
- [25] D. Chen, S. Aubry, G. P. Tsironis *Phys. Rev. Lett.* **77**, 4776 (1996).
- [26] S. Flach, C R Willis *Phys. Rep.* **295**, 181 (1998).
- [27] S. Flach, Private Communication.
- [28] M. Sato, B. E. Hubbard, A. J. Sievers *Rev. Mod. Phys.* **78** 137 (2006)
- [29] S. Baroni, S. D. Gironcoli, A. D. Corso, *Rev. Mod. Phys.* **73**, 515 (2001).
- [30] M. Lazzeri, S. D. Gironcoli *Phys. Rev. Lett.* **81**, 2096 (1998).
- [31] Ph. Ghosez, X. Gonze, J. P. Michenaud, *Ferroelectrics* **206-207**, 205 (1998).
- [32] Ph Ghosez, J P Michenaud, X Gonze *Phys. Rev. B* **52**, 6224 (1998).
- [33] M. H. Cohen, J. Ruvalds *Phys. Re. Lett.* **23**, 1378 (1969); J. Ruvalds, Private Communication.
- [34] C. J. Brennan, K. A. Nelson *J. Chem. Phys.* **107**, 9691 (1997).
- [35] B. Becker, P. K. Schelling, S. R. Phillpot *J. Appl. Phys.* **99**, 123715 (2006).
- [36] L. He, D. Vanderbilt *Phys. Rev. B* **68**, 134103 (2003).
- [37] J. P. Nguenang, R. A. Pinto, A. Flach *Phys. Rev. B* **75**, 214303 (2007).
- [38] S. Flach, A. V. Gorbach *Physics Reports* **467**, 1 (2008).
- [39] C. C. Marston, G. G. Balint-Kurti *J. Chem. Phys.* **91**, 3571 (1989).
- [40] Z. Ivic, G. P. Tsironis, *Physica D* **216**, 200 (2006).
- [41] V. Gopalan, T. E. Mitchell *J. Appl. Phys.* **83**, 941 (1997).
- [42] T. J. Yang, V. Gopalan, P. J. Swart, U. Mohideen *Phys. Rev. Lett.* **82** 4106 (1999).
- [43] T. Ueda, T. Y. Takai, R. Shimizu, H. Yagyu, T. Matsushima, M. Souma, *Japan. J. Appl. Phys. Part I* **39**, 1200 (2000).
- [44] N. Iyi, K. Kitamura, F. Izumi, K. J. Yamamoto, T. Hayashi, H. Asano, S. Kimura *J. Solid State Chem.* **101**, 340 (1992).
- [45] S. Kojima, *Japan. J. Appl. Phys. Part I* **32**, 4373 (1993).
- [46] J. Blumel, E. Born, T. Metzger *J. Phys. Chem. Solids* **55**, 589 (1994).
- [47] A. K. Bandyopadhyay, P. C. Ray, V. Gopalan *J. Appl. Phys.* **100**, 114106 (2006).

*Corresponding author: asisbanerjee1000@gmail.com, akbece12@yahoo.com